

RESEARCH

Open Access



Proteomics and lipidomics of human umbilical cord mesenchymal stem cells exposed to ionizing radiation

Dongmei Han¹, Li Ding¹, Xiaoli Zheng¹, Sheng Li¹, Hongmin Yan¹, Jing Liu¹ and Hengxiang Wang^{1*}

Abstract

Objectives Mesenchymal stem cell (MSC)-based therapies exhibit beneficial effects on various forms of tissue damage, including ionizing radiation-induced lesions. However, whether ionizing radiation affects the functions of human umbilical cord mesenchymal stem cells (hucMSCs) remains unclear. This study aimed to investigate the effect and possible mechanisms of ionizing radiation on the proliferation and differentiation of hucMSCs.

Methods The hucMSCs were divided into the 1 Gy group (exposure to a single dose (1 Gy) of X-ray radiation (1 Gy/min) for 14 days) and control (without radiation treatment) group. The proliferation, apoptosis, and adipogenic and osteogenic differentiation abilities of hucMSCs in the two groups were evaluated. Moreover, the lipidomics and proteomics analyses were conducted to explore crucial lipids and proteins by which ionizing radiation affected the functions of hucMSCs. In addition, the effects of BYSL on radiation-treated hucMSCs were explored, as well as the involved potential mechanisms.

Results X-ray radiation treatment inhibited proliferation, promoted apoptosis, and decreased adipogenic and osteogenic differentiation abilities of hucMSCs. Key lipids, such as triglyceride (TG) and phosphatidylcholine (PC), and hub proteins (BYSL, MRTO4, and RRP9) exhibited significant differences between the 1 Gy group and control group. Moreover, BYSL, MRTO4, and RRP9 were significantly correlated with TG and PC. BYSL overexpression evidently promoted the cell proliferation, adipogenic and osteogenic differentiation abilities of radiation-treated hucMSCs, as well as the protein expression levels of p-GSK-3 β /GSK-3 β and β -catenin, while suppressed cell apoptosis. However, the GSK-3 β inhibitor (1-Az) treatment reversed the protein expression levels of p-GSK-3 β /GSK-3 β , β -catenin and BYSL, as well as the cell proliferation, apoptosis, adipogenic and osteogenic differentiation abilities of radiation-treated hucMSCs.

Conclusions Our findings reveal that the proliferation and differentiation of hucMSCs are suppressed by radiation, which may be associated with the changes of key lipids (TG and PC) and proteins (BYSL, MRTO4, and RRP9). Furthermore, BYSL promotes adipogenic and osteogenic differentiation abilities of radiation-treated hucMSCs via GSK-3 β / β -catenin pathway. These findings help explain the response of hucMSCs to radiation and have clinical implications for improving the outcomes of MSC-based therapies after radiotherapy.

Keywords Ionizing radiation, Umbilical cord mesenchymal stem cells, Lipidomics, Proteomics, Adipogenic differentiation, Osteogenic differentiation

*Correspondence:
Hengxiang Wang
hematology123@163.com



Background

Radiation therapy is a highly efficient treatment for many cancers, including intensity-modulated radiation therapy, stereotactic radiotherapy, proton radiotherapy, etc. [1–3]. Various efforts such as dose escalation and altered fractionation have been done to improve the outcome [4]. However, the results are inconclusive owing to various obstacles such as radioresistance. In addition, dose escalation of radiation therapy can cause adverse complications to adjacent normal tissue and organs [5]. Ionizing radiation can lead to myelosuppression and hematopoietic damage, as well as radiotherapy obstacles [6–8]. In addition, ionizing radiation can cause acute radiation syndrome, which leads to damage of hematopoietic, gastrointestinal, and cerebrovascular systems [9]. Whole-body radiation of approximately 0.5–2 Gy can reduce the number of cells in hematopoietic organs, which can further lead to immune suppression and organ dysfunction [10]. Therefore, it is necessary to explore a reliable approach to treat radiation therapy-related side effects.

In preclinical studies, mesenchymal stem cell (MSC)-based therapies exhibit beneficial effects on various forms of tissue damage, including ionizing radiation-induced lesions [11, 12]. MSCs are defined as multipotent stem cells that possess the abilities to self-renew and differentiate into various cell types [13, 14]. Due to their regenerative properties and immunoregulatory functions, MSCs have attracted great interest for their potential in treating human diseases [15–17]. Notably, MSCs have shown potential to migrate to radiation-induced lesion sites and promote the regeneration of functional tissues by establishing a nurturing microenvironment [18]. Due to the regenerative capacities of MSCs, administration of exogenous MSCs to patients before or during radiation therapy has been proposed for treating acute radiation-induced side effects [19]. Nevertheless, the regenerative potential of this approach is associated with the radioresistance of the transplanted cells. In addition, ionizing radiation can affect the differentiation of various types of cells including MSCs. For example, radiation-induced osteocyte senescence decreases the differentiation potential of BMSCs [20]. Previous studies have shown that the phenotypic and immunoregulatory properties of human umbilical cord MSCs (hucMSCs) are similar to that of bone marrow MSCs (BMSCs) [21, 22]. Notably, compared to the other original MSCs, the hucMSCs take advantages in short amplification time, high proliferation rate, higher safety and convenience [23, 24]. Subsequently, Metheny et al. discovered that hucMSCs not only promoted the reestablishment of hematopoietic lineages in vivo, but also accelerated megakaryocyte proliferation over BMSCs [25]. Interestingly, Yang et al. have revealed that hucMSCs have more advantages

over BMSCs in restoring and promoting the recovery of radiation-induced hematopoietic damage [26]. In addition, Liu et al. found that hucMSCs could improve irradiation-induced skin ulcers healing of rat models [27]. These findings have confirmed that hucMSCs might have good potential to counteract radiation-induced damage. Despite these, the effects of ionizing radiation on MSCs from various sources, including hucMSCs, remains incompletely understood to date, let alone the underlying mechanisms.

It is reported that MSCs do not increase cell apoptosis after receiving ionizing radiation, but upregulate the expression of various genes involved in DNA damage response and DNA repair [28]. Interestingly, MSCs can maintain osteogenic and adipogenic differentiation abilities even after radiation [29]. Thus, this study was performed to explore the effect of ionizing radiation on the proliferation and differentiation of hucMSCs, as well as the adipogenic and osteogenic differentiation abilities, which are shown to have the advantages of non-invasive harvest procedure, low immunogenicity, easy expansion in vitro, and ethical accessibility compared to other sources of MSCs [30, 31]. Moreover, it is reported that transplanting human neural stem cells with half SOX9 gene dosage promotes tissue repair and functional recovery from severe spinal cord injury [32]. Zhang et al. have found that regulating the Crif1 or PKA/CREB signaling pathways can help control the adipogenic and differentiation abilities of BMSCs after radiation injury, thereby improving the hematopoietic microenvironment after radiation therapy [33]. Therefore, MSCs pre-treated with gene expression or signaling pathway inhibitors/activators may exhibit better tissue repair effects in resisting the side effects caused by radiation therapy. This makes it particularly important to explore the mechanisms involved in ionizing radiation on the proliferation and differentiation of hucMSCs, which might provide critical basis for treating irradiation-induced related side effects and have promising prospective in clinical application.

Lipidomics and proteomics can comprehensively analyze the composition, dynamic changes, and interactions of lipids and proteins in organisms, revealing their roles in disease occurrence, development, and treatment [34, 35]. Herein, we conducted the lipidomics and proteomics analyses to explore the possible mechanism by which ionizing radiation affected the functions of hucMSCs. Our finding will provide new data to support the clinical use of hucMSCs in radiation therapy.

Materials and methods

Cell culture

The hucMSCs were cultured in MEM- α [containing 10% fetal bovine serum (FBS; HyClone, Logan, UT, USA) and

1% antibiotics] and maintained in a 37 °C humidified incubator with 5% CO₂. The medium was changed every 2 days until the confluence of cells reached more than 80%. Then, the cells were passaged. Hoechst DNA staining, agar culture, and PCR did not show mycoplasma infection, as well as MycoAlert mycoplasma detection kit (LT07-218, LONZA, USA) detection. The first to the third passage of hucMSCs in the logarithmic growth stage were used for the subsequent experiments.

Characterization of hucMSCs

The morphology of hucMSCs was observed and photographed using a microscope (DMi3000 B, Leica, Germany). Moreover, the phenotype of hucMSCs was identified by detection of the phenotype markers (CD54, CD44, CD90, and CD34) by flow cytometry. In detail, hucMSCs were harvested and suspended with 1× PBS. The hucMSCs were then incubated with the corresponding antibodies for 30 min at the room temperature away from light. The supernatant was then removed by centrifugation at 1000 rpm for 5 min, and the cells were washed and suspended by 1× PBS. The surface markers were detected using the CytoFLEX S flow cytometer (Beckman Coulter, Fullerton, CA) and analyzed by CELL Quest software (BD Biosciences, San Jose, CA).

Adipogenic induction

The hucMSCs were cultured in a 37 °C, 5%CO₂ incubator. When hucMSCs reached 80–90% confluence, hucMSCs were digested by 0.25% trypsin–0.04% EDTA. Then, the hucMSCs at a density of 2×10^4 cells/cm² were inoculated into six-well plates and incubated with complete medium in a 37 °C, 5%CO₂ incubator. When the hucMSCs reached 100% confluence, the original culture supernatant was discarded. Following the manufacturer's instructions of the commercial adipogenic induction kits (HUXUC-90031, Cyagen, Guangzhou, China), the induction solution A and B were alternately added for adipogenic induction. When the lipid droplets appeared in the cells, culture was continued with the induction solution B until the lipid droplets were large and round enough. The cells were fixed with 4% neutral paraformaldehyde solution for 30 min, and stained with oil red O staining solution for 30 min. The adipocytes were observed under a microscope (DMi3000 B, Leica).

Osteogenic differentiation

The hucMSCs were cultured in a 37 °C, 5%CO₂ incubator. When hucMSCs reached 80–90% confluence, hucMSCs were digested by 0.25% trypsin–0.04% EDTA. Then, the hucMSCs at a density of 2×10^4 cells/cm² were inoculated into six-well plates pretreated with 0.1% gelatin and incubated with complete medium in a 37 °C, 5%CO₂

incubator. When the hucMSCs reached 60–70% confluence, the complete medium was replaced with hucMSCs osteogenic differentiation medium (HUXUC-90021, Cyagen, Guangzhou, China). Fresh differentiation medium was replaced every 3 days, and the culture lasted for 2–4 weeks. The induction was stopped, and the cells were fixed with 4% neutral paraformaldehyde solution for 30 min, and stained with alizarin red staining solution for 3–5 min. The osteoblasts were observed under a microscope (DMi3000 B, Leica).

Cell treatment and transfection

Numerous evidences indicated that 1–2 Gy typically does not cause large-scale apoptosis of MSCs, but it is sufficient to induce DNA damage, impaired differentiation potential, cell cycle arrest, and proliferation inhibition, making it easier to study the regulatory mechanisms of radiation on MSCs function [20, 36, 37]. In addition, it is reported that exposure to ionizing radiation as low as 1 Gy in whole or in part can cause acute radiation syndrome [38]. Thus, considering the induction of acute radiation syndrome and the radiation dose basis of hucMSCs, this study was conducted using the lowest dose (1 Gy) that causes acute radiation syndrome. To investigate the effect of radiation on hucMSCs differentiation, hucMSCs were divided into the 1 Gy group and control group. For the radiation treatment, hucMSCs were irradiated with 1 Gy (X-ray) at a rate of 1 Gy/minute, and hucMSCs without radiation treatment were used as controls. Lentiviral vectors of BYSL (oe-BYSL) and negative control oe-NC were constructed and transfected in radiation-treated hucMSCs. After transfection, lentivirus-infected hucMSCs were subjected to puromycin for selection. After selection, the stable transfected cells were identified, and expression of BYSL was confirmed by qRT-PCR and western blot analyses.

Cell counting Kit-8 (CCK-8) assay

The hucMSCs at logarithmic growth stage were collected, digested, centrifuged, and re-suspended with fresh complete medium. The hucMSCs suspension was inoculated into the 96-well plate, and cultured in a 37 °C, 5%CO₂. On days 7 and 14 of radiation treatment, CCK-8 solution (Beyotime, Jiangsu, China) was added to each well. After incubation for 2 h, the absorbance at 450 nm wavelength was measured using a micro-plate reader (DR-3518G, Wuxi Hiwell Diatek, China).

Flow cytometric analysis of apoptosis

The hucMSCs were digested by 0.25% trypsin without EDTA and washed with precooling PBS. Cells were lightly re-suspended with Annexin V-EGFP binding solution. Then, cells were successively stained with 5 μL

Annexin V-EGFP for 15 min and 10 μ L propidium iodide for 10 min at room temperature in the dark. Apoptotic cells were detected using the CytoFLEX S flow cytometer (Beckman Coulter) and analyzed by CELL Quest software (BD Biosciences).

Lipidomics analysis

Total lipid was extracted from cell samples from the 1 Gy group and control group ($n = 3$ in each group) as previously described by Matyash et al. [39]. Lipidomics analysis was then conducted performed on a Q Exactive Plus mass spectrometer (Thermo Scientific, USA) with a Vanquis UHPLC (Thermo Scientific). Mass spectrometry (MS) and tandem mass spectrometry (MS/MS) data were obtained in both positive and negative ion modes. Lipid identification was conducted using LipidMap (www.lipidmaps.org) was used for the identification and quantification of the lipid species based on the MS/MS data. Next, the search results from the individual positive or negative ion files from each sample group were aligned and merged for each annotated lipid. Resultant data was strictly manually checked to eliminate false positive based on the peak shake, adduct ions behavior, fragmentation pattern, and chromatographic behavior, respectively. For the multivariate statistical analysis, the lipid profiling of samples was analyzed using SIMCA (version 14.1) software. The significantly different components were determined based on the combination of a statistically significant threshold of variable influence on projection (VIP) values obtained from orthogonal partial least squares–discriminant analysis (OPLS–DA) and t -test (p value) on the raw data. The differential lipids were identified with the cutoff value of $p < 0.05$ and $VIP > 1$. To explore the disturbed lipid metabolic pathways, the Kyoto Encyclopedia of Genes and Genomes (KEGG) pathway enrichment analysis for differential lipids were performed using MetaboAnalyst [40]. The cutoff value was $p < 0.05$.

Proteomics analysis

To assess the proteome changes of hucMSCs in response to radiation, six cell samples from the 1 Gy group and control group ($n = 3$ in each group) were processed by data independent acquisition (DIA) individually. In brief, samples were lysed in lysis buffer for 30 min on ice and the concentration of protein supernatant was determined using the Bicinchoninic acid (BCA) method. The proteins were then prepared using the commercial iST Sample Preparation kit (PreOmics, Germany). The nano-high-performance liquid chromatography–tandem mass spectrometry (nano-HPLC–MS/MS) was performed. Samples were randomly loaded, and MS1 and MS2 data were collected. The iRT kit (Ki3002, Biognosys AG, Switzerland)

was utilized to calibrate the retention time of extracted peptide peaks. The obtained DIA data were subjected to data normalization and relative protein quantification using Spectronaut 17 (Biognosys AG, Switzerland). Spectronaut was set up to search the database of uniprot-homo sapiens assuming trypsin as the digestion enzyme. Retention time prediction type was set to dynamic iRT. Data extraction was determined by Spectronaut based on the extensive mass calibration. Spectronaut will determine the ideal extraction window dynamically depending on iRT calibration and gradient stability. Q value (FDR) cutoff on precursor level was 1% and protein level was 1%. Decoy generation was set to mutated which similar to scrambled but will only apply a random number of amino acid position swamps (min = 2, max = length/2). In the Spectronaut export file, empty values were replaced by Filtered ones, and all samples with hollow values accounting for more than 50% were removed. The remaining null values were filled with all sample minimums. Normalization strategy was set to Local normalization. The average top 3 filtered peptides which passed the 1% Q value cutoff were used to calculate the major group quantities. Differential expressed proteins (DEPs) were identified with the cutoff value of $p < 0.05$. To elucidate their biological function, Gene Ontology (GO) and KEGG pathway enrichment analysis was conducted using clusterProfiler package [41]. Disease ontology (DO) enrichment was also conducted using DOSE [42]. The cutoff value was $p < 0.05$.

Analysis of hub proteins and their correlation with differential lipids

The protein–protein interaction (PPI) relationships between DEPs were analyzed using the STRING database (version 11.5) [43, 44]. The PPI network was visualized using Cytoscape (version 3.6.1) [45]. The hub proteins in the PPI network were identified using MCODE plug-in. Moreover, the correlation between hub proteins and differential lipids was analyzed by Pearson Correlation analysis. The threshold value was $p < 0.01$ and $|\text{Correlation}| > 0.8$.

QRT-PCR

Total RNA was extracted from hucMSCs using TRIzol reagent (Invitrogen, USA). FastKing gDNA Dispelling RT SuperMix (TIANGEN, China) was used to synthesize cDNA. Then qRT-PCR was performed using SYBR Green PCR Master Mix (Lifeint, China) and CFX96 Touch Real-Time PCR Detection System (Bio-Rad, USA). GAPDH were used as internal controls. The PCR primers used in the present study were as follows: BYSL, forward 5'-AGG AAA AAC ATG CGC CCC T-3', reverse 5'-TGC TTG CTG CAA AAT CCG TC-3'; MRTO4, forward 5'-ACA

GAA ATG GAC TAC GCC CG-3', reverse 5'-CCT CCT TGC ACA CCT CGT AG-3'; RRP9, forward 5'-GAC ATT CGC GTT TTA CGG GG-3', reverse 5'-TCT CTG CCA CAT TCC ACA CC-3'; and GAPDH, forward 5'-GAA GGT CGG AGT CAA CGG AT-3' and reverse 5'-CTT CCC GTT CTC AGC CAT GT-3'. The thermocycling conditions comprised one cycle at 95 °C for 10 min, followed by 40 cycles of amplification (95 °C for 12 s and 60 °C for 40 s). Fold-changes in mRNA expression were calculated using the $2^{-\Delta\Delta C_t}$ method.

Protein extraction and western blot

Cells were washed in PBS and lysed in RIPA lysate (P0013B, Beyotime, China) to obtain whole-cell protein, which were separated on SDS-PAGE and transferred to PVDF membranes. The membranes were incubated with primary antibodies against BYSL (1:1000; A11993, ABclonal, China), GSK-3 β (1:1000; AF5016, Affinity, China), p-GSK-3 β (1:1000; AF2016, Affinity, China), β -catenin (1:1000; AF6266, Affinity, China), GAPDH (1:1000; AF7021, Affinity, China) at 4 °C overnight. Then the membranes were incubated with HRP-conjugated secondary antibodies for 2 h at room temperature. Finally, the blots were developed with an enhanced Electrochemical luminescence (ECL) reagent (P1000, APPLYGEN, China). Images were analyzed using ImageJ (National Institutes of Health, Bethesda, MD).

Statistical analysis

All experimental data are presented as the means \pm standard deviation. The *t*-test compares the differences of two groups. The differences between groups were analyzed by one-way ANOVA in the GraphPad 7.0 software (La Jolla, California). The value of $p < 0.05$ indicated significant results.

Results

Characterization and differentiation abilities of hucMSCs

The morphology of hucMSCs was observed under microscope. We observed that hucMSCs exhibited a fibroblast-like, spindle-shaped morphology and adherent growth (Fig. 1A). Moreover, the results of flow cytometry revealed that most cells were highly positive for CD44 and CD90 (all > 98%) and negative for CD34 and CD45 (all < 1%) (Fig. 1B). Therefore, the cells were confirmed as hucMSCs. Furthermore, obvious lipid droplets were observed by oil red O staining, indicating that the hucMSCs were successfully differentiated into adipocytes in vitro (Fig. 1C). In addition, alizarin red staining showed positive calcium nodules, indicating that hucMSCs had osteogenic differentiation ability (Fig. 1D).

Radiation inhibited proliferation, promoted apoptosis, and decreased adipogenic and osteogenic differentiation abilities of hucMSCs

The effect of radiation on the proliferation, apoptosis, and decreased adipogenic and osteogenic differentiation abilities of hucMSCs were investigated. We first observed the morphology of hucMSCs after radiation treatment. As results, the hucMSCs in the control group were spindle-shaped, adherent to the wall, with equal cytoplasmic content and oval-shaped nuclei. In the 1 Gy group, the hucMSCs were short spindle-shaped after 7 days of radiation treatment, and they had larger cell bodies and more particles after 14 days of radiation treatment (Fig. 2A). The results of CCK-8 assay revealed that the cell viability of the 1 Gy group was dramatically lower than that of the control group after 7 and 14 days of radiation treatment ($p < 0.01$, Fig. 2B), indicating that radiation inhibited hucMSCs proliferation. The results of flow cytometry demonstrated that radiation treatment caused an obvious increase in cell apoptosis ($p < 0.01$, Fig. 2C). Moreover, obvious lipid droplets were observed by oil red O staining, and the number of lipid droplets in the 1 Gy group was clearly lower than that in the control group (Fig. 2D), indicating that radiation treatment inhibited the adipogenic differentiation abilities of hucMSCs. Furthermore, alizarin red staining revealed that the positive calcium nodules of the 1 Gy group was visibly lower than that in the control group (Fig. 2E), manifesting that radiation treatment inhibited the osteogenic differentiation abilities of hucMSCs.

Identification of differential lipids and enrichment analysis

To explore whether lipid metabolism of hucMSCs was affected by radiation, we conducted lipidomics analysis to evaluate the lipid composition changes of hucMSCs under radiation. With the cutoff value of $p < 0.05$ and VIP > 1, a total of 462 differential lipids were identified between the control and 1 Gy groups, including 299 up-regulated lipids and 163 down-regulated lipids (Fig. 3A). The heatmap of the top 50 significant differential lipids is shown in Fig. 3B. Furthermore, these differential lipids were found to be significantly enriched in pathways, such as glycerophospholipid metabolism, sphingolipid metabolism, and linoleic acid metabolism (Fig. 3C). In addition, Fig. 3D reveals that the expression levels of key lipids shown significant differences between 1 Gy and control groups (all $p < 0.05$).

Identification of DEPs and enrichment analysis

To explore the proteome changes of hucMSCs in response to radiation, we conducted proteomics analysis. A total of 718 DEPs (276 up-regulated and 442

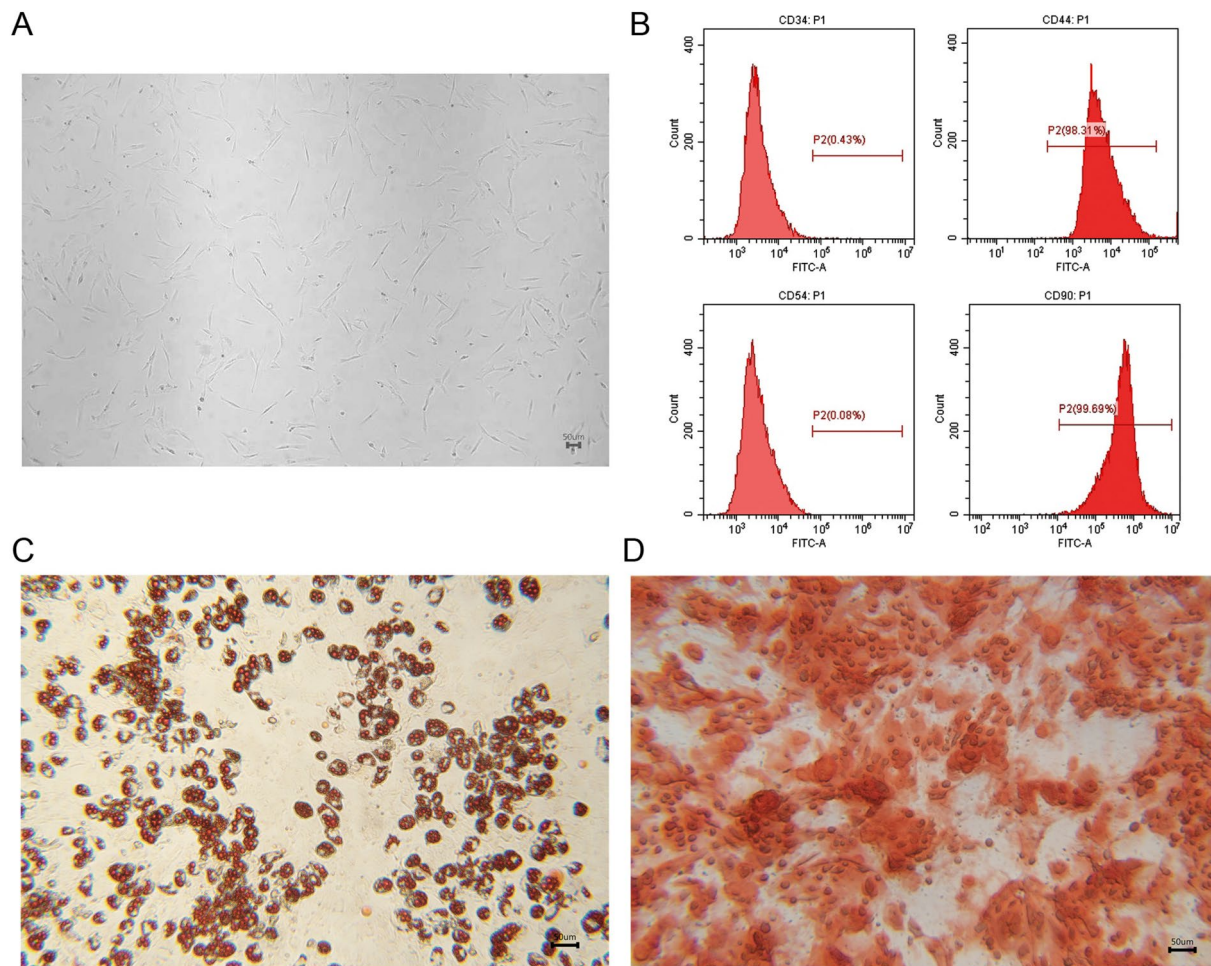


Fig. 1 Characterization and differentiation abilities of hucMSCs. **A** Morphology of hucMSCs. **B** Cell markers were analyzed by flow cytometry. **C** Adipogenic differentiation abilities of hucMSCs were evaluated by oil red O staining. **D** Osteogenic differentiation abilities of hucMSCs were assessed with alizarin red staining. Scale: 50 μ m. HucMSCs: human umbilical cord MSCs

down-regulated) were identified between the control and 1 Gy groups (Fig. 4A). The expression heatmap of the top 50 significant DEPs is shown in Fig. 4B. Subsequent functional enrichment analyses revealed that the DEPs were significantly enriched in 124 GO terms and 33 KEGG pathways. For instance, the overrepresented GO terms included ribonucleoprotein complex biogenesis, regulation of DNA metabolic process, and ribosome biogenesis (Fig. 4C); the significant pathways included hsa03030: DNA replication, hsa04350: TGF-beta signaling pathway, and hsa03010: Ribosome (Fig. 4D). In addition, DO enrichment showed that DEPs were mainly related to connective tissue cancer and bone sarcoma (Fig. 4E).

Correlation analysis of DEPs and differential lipids

Using the STRING database, we searched the PPI relationships between DEPs and constructed a PPI network including 3654 pairs. Then, 40 hub proteins were

identified from the PPI network based on MCODE score (Fig. 5A). By further correlation analysis, 32 DEPs and 20 differential lipids were screened and their correlation network is displayed in Fig. 5B. Among the 20 differential lipids, 14 lipids were upregulated in the 1 Gy group compared to those in the control group, and 6 lipids were downregulated ($p < 0.05$; Fig. 3D). Top 10 hub DEPs were selected from 32 DEPs by the descending order of degree, MNC, and MCC in the CytosHubba plug-in (Fig. 5C). Finally, three hub proteins (BYSL, MRTO4, and RRP9) were screened out by intersecting top 10 DEPs according to degree, MNC, and MCC (Fig. 5C). Proteomics analysis and qRT-PCR both identified the downregulation of BYSL, MRTO4, and RRP9 in the 1 Gy group compared to those in the control group ($p < 0.05$; Fig. 6A and B). Correlation analysis showed that BYSL was positively related to triglyceride (TG) and negatively related to phosphatidylethanolamine (PE), Phosphatidylcholine (PC), and

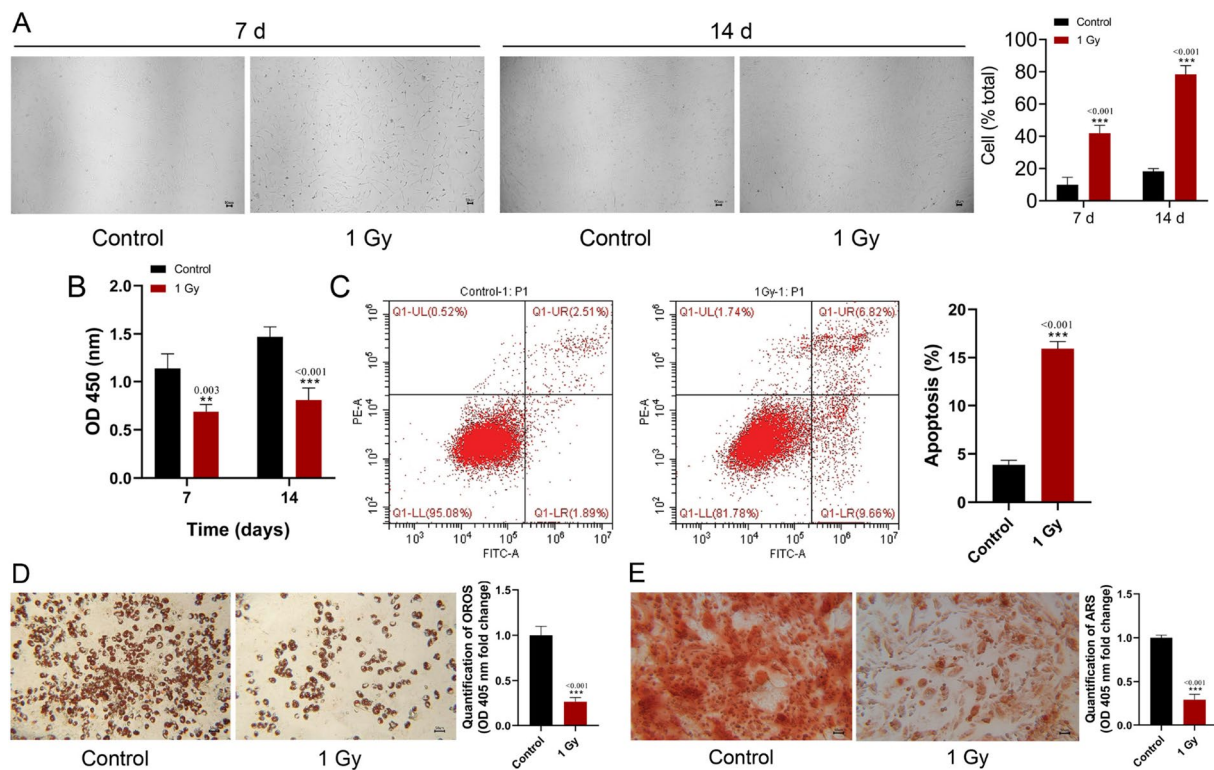


Fig. 2 Radiation inhibited proliferation, promoted apoptosis, and decreased adipogenic and osteogenic differentiation abilities of hucMSCs. The hucMSCs were divided into the 1 Gy group and control group. **A** Morphology of hucMSCs in different groups. **B** Cell proliferation of different groups was detected by CCK-8 assay. **C** Cell apoptosis of different groups was detected by flow cytometry. **D** Adipogenic differentiation abilities of hucMSCs in different groups were evaluated by oil red O staining. **E** Osteogenic differentiation abilities of hucMSCs in different groups were assessed with alizarin red staining. Scale: 50 μ m. ** $p < 0.01$, *** $p < 0.001$ compared to control group. HucMSCs: human umbilical cord MSCs

MePC (Fig. 6C). MRTO4 was positively related to TG and negatively related to sphingomyelin (SM), PC, and MePC (Fig. 6C). RRP9 was negatively related to SM, PE, and PC (Fig. 6C).

BYSL promotes adipogenic and osteogenic differentiation abilities of radiation-treated hucMSCs via GSK-3 β / β -catenin pathway

It is reported that overexpression of BYSL increases the activity of GSK-3 β / β -catenin signaling pathway [46], and GSK-3 β / β -catenin pathway facilitates the osteogenic differentiation abilities of MSCs [47]. However, few studies reported the relationships between MRTO4, RRP9 and differentiation abilities of MSCs. Thus, this study was further explored the whether BYSL promotes adipogenic and osteogenic differentiation abilities of hucMSCs after radiation treatment via GSK-3 β / β -catenin pathway. To elucidate the BYSL in radiation-treated hucMSCs, the lentiviral vector of BYSL (oe-BYSL) was constructed and transfected in radiation-treated hucMSCs, and the transfection efficiency were measured (Fig. 7A and B). Interestingly, BYSL overexpression evidently promoted radiation-treated hucMSCs proliferation ($p <$

0.05; Fig. 7C), while suppressed cell apoptosis ($p < 0.01$; Fig. 7D). Notably, the BYSL upregulation significantly elevated the adipogenic and osteogenic differentiation abilities of radiation-treated hucMSCs (all $p < 0.01$; Fig. 7E and F). Besides, the protein expression levels of p-GSK-3 β /GSK-3 β and β -catenin in nuclear were obviously plummeted after radiation treatment, while BYSL overexpression reversed this trend (all $p < 0.05$; Fig. 8A). Furthermore, the GSK-3 β inhibitor (1-Az) was further added, and the results shown that 1-Az treatment reversed the protein expression levels of p-GSK-3 β /GSK-3 β , β -catenin and BYSL, as well as the cell proliferation, apoptosis, adipogenic and osteogenic differentiation abilities of radiation-treated hucMSCs (all $p < 0.05$; Fig. 8B–F). All these data indicated that BYSL promotes adipogenic and osteogenic differentiation abilities of radiation-treated hucMSCs via GSK-3 β / β -catenin pathway.

Discussion

In this study, we examined the effect of ionizing radiation on the proliferation and differentiation of hucMSCs and then explored the underlying mechanisms

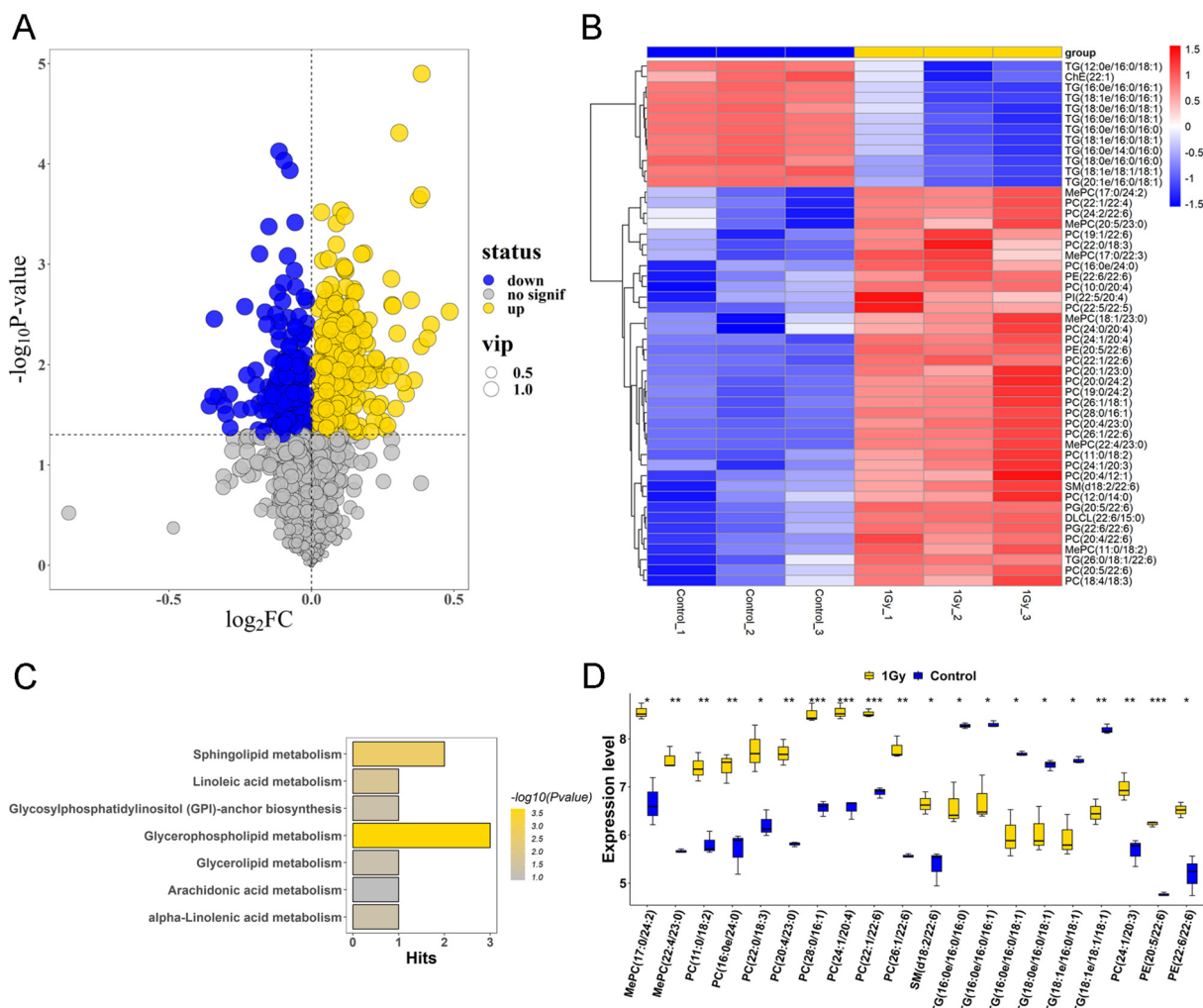


Fig. 3 Identification of differential lipids and enrichment analysis. **A** Volcano plot of differential lipids between the 1 Gy and control groups. **B** Expression heatmap of the top 50 differential lipids. **C** Pathway enrichment results of differential lipids. **D** Expression levels of key lipids between 1 Gy and control groups. * $p < 0.05$, ** $p < 0.01$

through proteomics and lipidomics analyses. We found that radiation treatment inhibited proliferation, promoted apoptosis, and decreased adipogenic and osteogenic differentiation abilities of hucMSCs. Key lipids, including TG and PC, and hub proteins (BYSL, MRTO4, and RRP9) exhibited significant differences between the 1 Gy and control groups. These macromolecules may be key mechanisms regulating the functions of hucMSCs after radiation. Besides, we also found that BYSL promotes adipogenic and osteogenic differentiation abilities of radiation-treated hucMSCs via GSK-3 β / β -catenin pathway.

Radiation therapy is an effective treatment option for many cancers but can cause immune suppression and organ injury. MSCs have a high capacity for self-renewal and multipotent differentiation, which are under investigation to treat radiation-induced organ injury [48]. MSCs

are capable of interacting with cells of immune systems and migrate to injured sites to decrease the production of pro-inflammatory cytokines and improve the survival of damaged cells [49]. However, a previous study has revealed that radiation decreased the osteogenic differentiation potential of BMSCs due to DNA damage and senescence caused by radiation (24). Zhang et al. demonstrated that radiation suppressed the osteogenic differentiation and enhanced adipogenic differentiation of BMSCs, and overexpression of Crif1 promoted adipogenesis after radiation exposure [33]. Consistent with these findings, we found that hucMSCs were influenced by radiation and their proliferation and adipogenic and osteogenic differentiation abilities were suppressed after radiation exposure. Therefore, it is necessary to explore the key mechanisms mediating the biological response of MSCs to ionizing radiation, which may lead to the

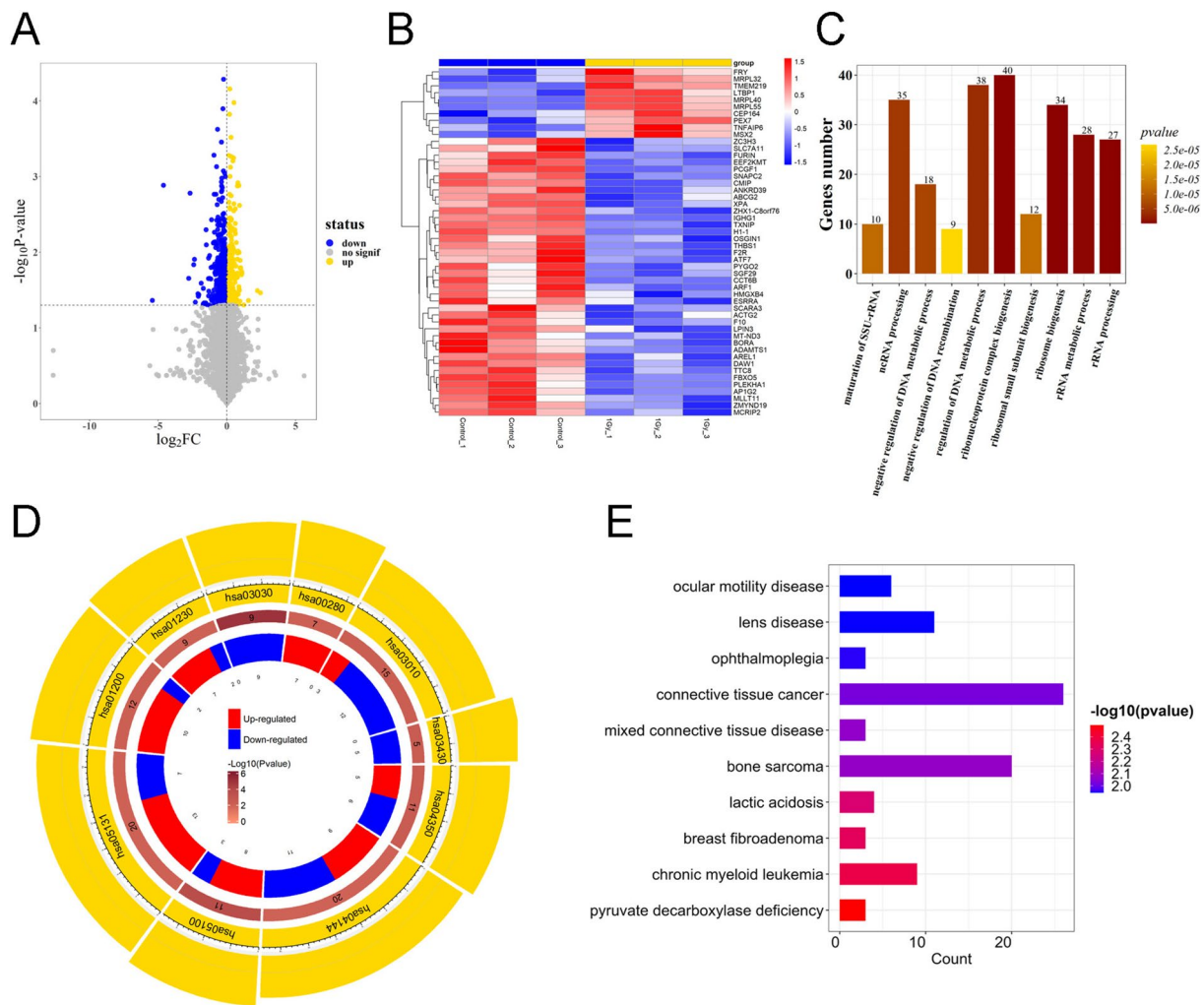


Fig. 4 Proteomics analysis for identification of DEPs between the 1 Gy and control groups. **A** Volcano plot of DEPs between the two groups. **B** Expression heatmap of the top 50 DEPs. **C** Histogram of the top 10 GO terms enriched by DEPs. **D** Loop graph of the top 10 KEGG pathways enriched by DEPs. **E** Top 10 DO enrichment terms enriched by DEPs

development of improved treatment strategies for stem cell therapy and cancer.

It is reported that cellular exposure to ionizing radiation can alter the atomic structure of target macromolecules, such as lipids and proteins via induction of oxidizing events and production of water radiolysis [50]. Since lipid droplet formation is a hallmark of adipogenic differentiation, lipidomics is able to reflect elevated lipid content and provides information on the adipogenic differentiation of MSCs. Previous studies on the MSC-based therapy for several metabolic diseases such as non-alcoholic fatty liver disease and type II diabetic diseases have revealed that MSCs may prevent disease progression via modulating lipid metabolism [51, 52]. In this study, key lipids were identified, and these differential lipids were found to be significantly enriched in pathways, such as glycerophospholipid metabolism, sphingolipid

metabolism, and linoleic acid metabolism. Alterations in sphingolipid metabolism have been described in multiple diseases, including neurodegeneration, cancer, chronic inflammation [53–55]. Linoleic acid is the most abundant polyunsaturated fatty acid in human nutrition, and the content of linoleic acid is closely related to various diseases, but excessive or metabolic imbalance may promote inflammation and chronic diseases [56, 57]. In addition, Campos et al. revealed that the lipid molecular profile of MSCs significantly changed after pro-inflammatory stimulation, with the PC species with shorter fatty acids (FAs) decreasing [58]. Levental et al. demonstrated that the PC was obviously increased in osteoblast plasma membranes relative to undifferentiated MSCs [59], indicating that PC change was associated with the osteogenic differentiation of MSCs. In addition, FAs are considered as energy storage in the form of TG in lipid droplets. TG is found to

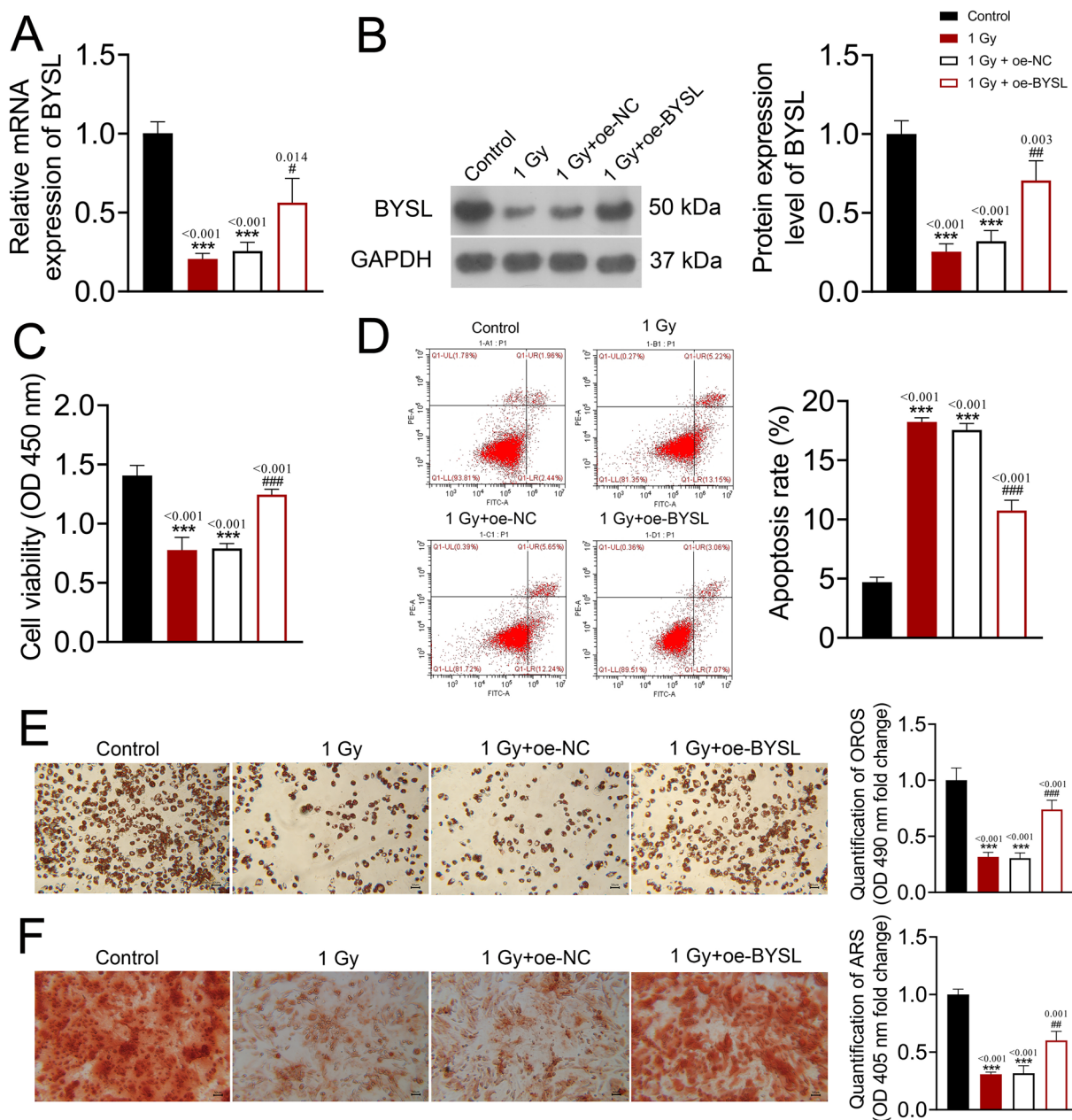


Fig. 7 Effects of BYSL overexpression on radiation-treated hucMSCs. **A** qRT-PCR measured the mRNA expression of BYSL. **B** Western blot analysis detected the protein expression of BYSL. **C** Cell proliferation detected using CCK-8 assay. **D** Cell apoptosis detected using flow cytometric analysis. Adipogenic (**E**) and osteogenic (**F**) differentiation abilities of radiation-treated hucMSCs after BYSL upregulation. Scale: 50 μ m. * p < 0.05, ** p < 0.01, *** p < 0.001 compared to control group; # p < 0.05, ## p < 0.01, ### p < 0.001 compared to 1 Gy + oe-NC group

be significantly upregulated in the adipogenic differentiation of MSCs [60], suggesting that TG is a key indicator for evaluating adipogenic differentiation of MSCs. In this study, PC and TG were identified as main lipids in hucMSCs that were dramatically affected by radiation exposure. Therefore, we conclude that detecting the level of PC and TG may be used to reflect the biological response

of hucMSCs to ionizing radiation and guide the repair of hematopoietic damage during radiotherapy.

Furthermore, the proteomics enables to monitor key proteins that regulate functional changes of MSCs under different conditions. We thus conducted proteomics analysis to explore the action mechanism of radiation on hucMSCs. By further integration analysis

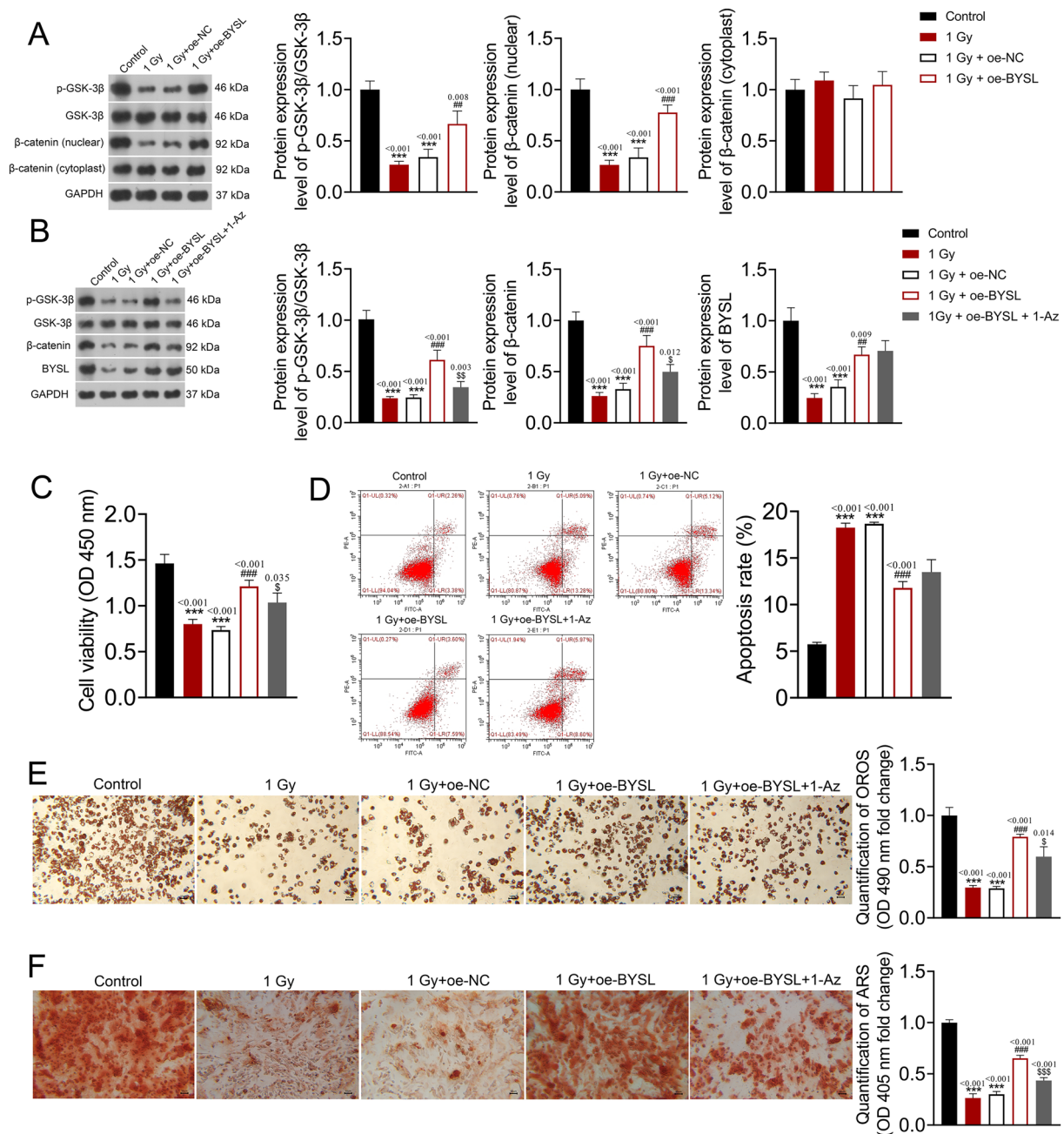


Fig. 8 BYSL promotes adipogenic and osteogenic differentiation abilities of radiation-treated hucMSCs via GSK-3β/β-catenin pathway. **A** Western blot analyses detected the protein expression levels of p-GSK-3β/GSK-3β and β-catenin after BYSL overexpression. **B** Western blot analyses detected the protein expression levels of p-GSK-3β/GSK-3β and β-catenin after BYSL overexpression and inhibitor of GSK-3β (1-Az) treatment. **C** Cell proliferation detected using CCK-8 assay. **D** Cell apoptosis detected using flow cytometric analysis. Adipogenic (**E**) and osteogenic (**F**) differentiation abilities of radiation-treated hucMSCs after BYSL upregulation. Scale: 50 μm. **p* < 0.05 compared to control group; #*p* < 0.05, ###*p* < 0.001 compared to 1 Gy + oe-NC group; §*p* < 0.05, §§*p* < 0.01, §§§*p* < 0.001 compared to 1 Gy + oe-BYSL group

with lipidomics data, we found that three downregulated hub proteins in the 1 Gy group, namely, BYSL, MRTO4, and RRP9. BYSL, coding for the human bys-tin protein, is a sensitive marker for astrocyte proliferation in brain damage and inflammation [61].

MRTO4 encodes a protein sharing a low level of sequence similarity with ribosomal protein P0. While the precise function of MRTO4 is currently unknown, it appears to be involved in mRNA turnover and ribosome assembly. Ribosome-related gene sets were

enriched in aldehyde dehydrogenase (ALDH) activity. High ALDH activity is a useful marker for identifying subpopulations in ADSCs with adipogenic and osteogenic differentiation potential, suggesting the importance of ribosome for differentiation of ADSCs [62]. RRP9 is a U3 small nucleolar protein essential for ribosome formation, which also has potential to regulate adipogenic and osteogenic differentiation of MSCs [63]. Our correlation analysis revealed that BYSL was positively related to TG and negatively related to PE, PC, and MePC in 1 Gy-treated hucMSCs. MRTO4 was positively related to TG and negatively related to SM, PC, and MePC. RRP9 was negatively related to SM, PE, and PC. These results confirmed the potential regulation of BYSL, MRTO4, and RRP9 on adipogenic osteogenic differentiation of hucMSCs after radiation. BYSL can enhanced the GSK-3 β / β -Catenin signaling pathway to promote glioblastoma cell migration, invasion, and mesenchymal transition [46]. The downregulation of GSK-3 β / β -Catenin signaling inhibits the adipogenic and promotes the osteogenic differentiation of human ADSCs [64]. Herein, we also found that BYSL overexpression evidently promoted the cell proliferation, adipogenic and osteogenic differentiation abilities of radiation-treated hucMSCs, as well as the protein expression levels of p-GSK-3 β /GSK-3 β and β -catenin, while suppressed cell apoptosis. However, the GSK-3 β inhibitor (1-Az) treatment reversed the protein expression levels of p-GSK-3 β /GSK-3 β , β -catenin and BYSL, as well as the cell proliferation, apoptosis, adipogenic and osteogenic differentiation abilities of radiation-treated hucMSCs. All these data indicated that BYSL promotes adipogenic and osteogenic differentiation abilities of radiation-treated hucMSCs via GSK-3 β / β -catenin pathway, and BYSL might be a potential target of MSC-based therapies for mitigating radiation-induced damage.

However, some limitations should be considered in this study. First, further investigation with systematic experiments is required to determine the effect of BYSL in the treatment of radiation-induced damage in the clinical. Besides, hucMSCs pre-treated with BYSL overexpression may exhibit better tissue repair effects in resisting the side effects caused by radiation therapy, which needs to be further validated in subsequent study. In addition, the functional validation and involved potential molecular mechanisms of MRTO4 and RRP9 in radiation-treated hucMSCs needed deeply investigated, as well as TG and PC. Finally, the differences between the experimental model and the clinical actual situation should also be considered, such as the impact of the complex in vivo microenvironment on the radiation response of hucMSCs.

Conclusion

Our findings reveal that the proliferation and differentiation of hucMSCs are suppressed by radiation, which may be associated with the changes of key lipids (TG and PC) and down-regulation of hub proteins (BYSL, MRTO4, and RRP9). Besides, BYSL promotes adipogenic and osteogenic differentiation abilities of radiation-treated hucMSCs via GSK-3 β / β -catenin pathway. These findings help explain the response of hucMSCs to radiation and offer potential target of MSC-based therapies for mitigating radiation-induced damage. However, these results are preliminary, and hucMSCs still face some challenges in mitigating the side effects of ionizing radiation, such as safety, efficacy stability, dosage, etc., and further research is needed.

Abbreviations

MSC	Mesenchymal stem cell
BCA	Bicinchoninic acid
BMSCs	Bone marrow MSCs
CCK-8	Cell Counting Kit-8
DEPs	Differential expressed proteins
DIA	Data independent acquisition
ECL	Electrochemical luminescence
FBS	Fetal bovine serum
GO	Gene Ontology
hucMSCs	Human umbilical cord mesenchymal stem cells
KEGG	Kyoto Encyclopedia of Genes and Genomes
nano-HPLC-MS/MS	Nano-high-performance liquid chromatography-tandem mass spectrometry
OPLS-DA	Orthogonal partial least squares-discriminant analysis
PC	Phosphatidylcholine
PPI	Protein-protein interaction
TG	Triglyceride
VIP	Variable influence on projection

Acknowledgements

Not applicable.

Author contributions

Conception and design of the research: D.H., L.D., H.W.; Acquisition of data: D.H., L.D., X.Z., S.L.; Analysis and interpretation of data: X.Z., H.Y., J.L., H.W.; Statistical analysis: D.H., L.D., J.L.; Drafting the manuscript: D.H., L.D.; Revision of manuscript for important intellectual content: H.W. All authors read and approved the final manuscript.

Funding

Not applicable.

Availability of data and materials

No datasets were generated or analysed during the current study.

Declarations

Ethics approval and consent to participate

Not applicable.

Consent for publication

Not applicable.

Competing interests

The authors declare no competing interests.

Author details

¹Department of Hematology, Air Force Medical University, Air Force Medical Center, PLA, No.30, Fucheng Road, Beijing 100142, China.

Received: 8 March 2025 Accepted: 10 April 2025

Published online: 28 April 2025

References

- Bourbonne V, Thureau S, Pradier O, Antoni D, Lucia F. Stereotactic radiotherapy for ultracentral lung tumours. *Cancer Radiother.* 2023;27(6–7):659–65.
- Mohan R. Intensity-modulated radiation therapy - you can have your cake and eat it too! *Med Phys.* 2023;50(Suppl 1):74–9.
- Dell'Oro M, Short M, Wilson P, Bezak E. Normal tissue tolerance amongst paediatric brain tumour patients- current evidence in proton radiotherapy. *Crit Rev Oncol/Hematol.* 2021;164:103415.
- Bradley JD, Paulus R, Komaki R, et al. Standard-dose versus high-dose conformal radiotherapy with concurrent and consolidation carboplatin plus paclitaxel with or without cetuximab for patients with stage IIIA or IIIB non-small-cell lung cancer (RTOG 0617): a randomised, two-by-two factorial phase 3 study. *Lancet Oncol.* 2015;16(2):187–99.
- Costa S, Reagan MR. Therapeutic irradiation: consequences for bone and bone marrow adipose tissue. *Front Endocrinol.* 2019;10:587.
- Li F, Zhang R, Hu C, et al. Irradiation haematopoiesis recovery orchestrated by IL-12/IL-12Rβ1/TYK2/STAT3-initiated osteogenic differentiation of mouse bone marrow-derived mesenchymal stem cells. *Front Cell Dev Biol.* 2021. <https://doi.org/10.3389/fcell.2021.729293>.
- Cao X, Wu X, Frassica D, et al. Irradiation induces bone injury by damaging bone marrow microenvironment for stem cells. *Proc Natl Acad Sci.* 2011;108(4):1609–14.
- Greenberger JS, Epperly M, editors. Bone marrow-derived stem cells and radiation response. In: *Seminars in radiation oncology*. Amsterdam: Elsevier; 2009.
- Guo H, Chou W-C, Lai Y, et al. Multi-omics analyses of radiation survivors identify radioprotective microbes and metabolites. *Science.* 2020;370(6516): eaay9097.
- Kumar A, Choudhary S, Kumar S, et al. Role of melatonin mediated G-CSF induction in hematopoietic system of gamma-irradiated mice. *Life Sci.* 2022;289:120190.
- Williams AR, Hare JM. Mesenchymal stem cells: biology, pathophysiology, translational findings, and therapeutic implications for cardiac disease. *Circ Res.* 2011;109(8):923–40.
- Nicolay NH, Rühle A, Perez RL, et al. Mesenchymal stem cells are sensitive to bleomycin treatment. *Sci Rep.* 2016;6(1):26645.
- Lin T, Yang Y, Chen X. A review of the application of mesenchymal stem cells in the field of hematopoietic stem cell transplantation. *Eur J Med Res.* 2023;28(1):268.
- Yamada A, Kitano S, Matsusaki M. Cellular memory function from 3D to 2D: three-dimensional high density collagen microfiber cultures induce their resistance to reactive oxygen species. *Mater Today Bio.* 2024;26:101097.
- Saadh MJ, Mikhailova MV, Rasoolzadegan S, et al. Therapeutic potential of mesenchymal stem/stromal cells (MSCs)-based cell therapy for inflammatory bowel diseases (IBD) therapy. *Eur J Med Res.* 2023;28(1):47.
- Lee S, Choe G, Yi J, et al. ROS-scavenging ultrasonicated graphene oxide/alginate microgels for mesenchymal stem cell delivery and hindlimb ischemia treatment. *Mater Today Bio.* 2024;29:101289.
- Mao Y, Liu P, Wei J, et al. Exosomes derived from Umbilical cord mesenchymal stem cell promote hair regrowth in C57BL6 mice through upregulation of the RAS/ERK signaling pathway. *J Transl Internal Med.* 2024;12(5):478–94.
- Nedeau AE, Bauer RJ, Gallagher K, et al. A CXCL5-and bFGF-dependent effect of PDGF-B-activated fibroblasts in promoting trafficking and differentiation of bone marrow-derived mesenchymal stem cells. *Exp Cell Res.* 2008;314(11–12):2176–86.
- Schmidt M, Haagen J, Noack R, et al. Effects of bone marrow or mesenchymal stem cell transplantation on oral mucositis (mouse) induced by fractionated irradiation. *Strahlenther Onkol.* 2014;190(4):399.
- Xu L, Wang Y, Wang J, et al. Radiation-induced osteocyte senescence alters bone marrow mesenchymal stem cell differentiation potential via paracrine signaling. *Int J Mol Sci.* 2021;22(17):9323.
- Liu Y, Chen XH, Si YJ, et al. Reconstruction of hematopoietic inductive microenvironment after transplantation of VCAM-1-modified human umbilical cord blood stromal cells. *PLoS ONE.* 2012;7(2): e31741.
- Liu Y, Yi L, Zhang X, et al. Cotransplantation of human umbilical cord blood-derived stromal cells enhances hematopoietic reconstitution and engraftment in irradiated BABL/c mice. *Cancer Biol Ther.* 2011;11(1):84–94.
- Baksh D, Yao R, Tuan RS. Comparison of proliferative and multilineage differentiation potential of human mesenchymal stem cells derived from umbilical cord and bone marrow. *Stem Cells.* 2007;25(6):1384–92.
- Fong CY, Richards M, Manasi N, Biswas A, Bongso A. Comparative growth behaviour and characterization of stem cells from human Wharton's jelly. *Reprod Biomed Online.* 2007;15(6):708–18.
- Metheny L, Eid S, Lingas K, et al. Posttransplant intramuscular injection of PLX-R18 mesenchymal-like adherent stromal cells improves human hematopoietic engraftment in a murine transplant model. *Front Med.* 2018;5:37.
- Yang SJ, Wang XQ, Jia YH, et al. Human umbilical cord mesenchymal stem cell transplantation restores hematopoiesis in acute radiation disease. *Am J Transl Res.* 2021;13(8):8670–82.
- Liu Z, Yu D, Xu J, et al. Human umbilical cord mesenchymal stem cells improve irradiation-induced skin ulcers healing of rat models. *Biomed Pharmacother.* 2018;101:729–36.
- Nicolay NH, Sommer E, Lopez R, et al. Mesenchymal stem cells retain their defining stem cell characteristics after exposure to ionizing radiation. *Int J Radiat Oncol Biol Phys.* 2013;87(5):1171–8.
- Nicolay NH, Lopez Perez R, Saffrich R, Huber PE. Radio-resistant mesenchymal stem cells: mechanisms of resistance and potential implications for the clinic. *Oncotarget.* 2015;6(23):19366–80.
- Li T, Xia M, Gao Y, Chen Y, Xu Y. Human umbilical cord mesenchymal stem cells: an overview of their potential in cell-based therapy. *Expert Opin Biol Ther.* 2015;15(9):1293–306.
- Xie Q, Liu R, Jiang J, et al. What is the impact of human umbilical cord mesenchymal stem cell transplantation on clinical treatment? *Stem Cell Res Therapy.* 2020;11:1–13.
- Liu JA, Tam KW, Chen YL, et al. Transplanting human neural stem cells with ≈50% reduction of SOX9 gene dosage promotes tissue repair and functional recovery from severe spinal cord injury. *Adv Sci.* 2023;10(20): e2205804.
- Zhang X, Xiang L, Ran Q, et al. Crif1 promotes adipogenic differentiation of bone marrow mesenchymal stem cells after irradiation by modulating the PKA/CREB signaling pathway. *Stem Cells.* 2015;33(6):1915–26.
- Nurmohamed NS, Kraaijenhof JM, Mayr M, et al. Proteomics and lipidomics in atherosclerotic cardiovascular disease risk prediction. *Eur Heart J.* 2023;44(18):1594–607.
- Xu J, Bankov G, Kim M, et al. Integrated lipidomics and proteomics network analysis highlights lipid and immunity pathways associated with Alzheimer's disease. *Transl Neurodegen.* 2020;9(1):36.
- Iwasa M, Fujii S, Fujishiro A, et al. Impact of 2 Gy γ-irradiation on the hallmark characteristics of human bone marrow-derived MSCs. *Int J Hematol.* 2021;113(5):703–11.
- Bai J, Wang Y, Wang J, et al. Irradiation-induced senescence of bone marrow mesenchymal stem cells aggravates osteogenic differentiation dysfunction via paracrine signaling. *Am J Physiol Cell Physiol.* 2020;318(5):C1005–C1017.
- López M, Martín M. Medical management of the acute radiation syndrome. *Rep Pract Oncol Radiother.* 2011;16(4):138–46.
- Matyash V, Liebisch G, Kurzchalia TV, Shevchenko A, Schwudke D. Lipid extraction by methyl-tert-butyl ether for high-throughput lipidomics. *J Lipid Res.* 2008;49(5):1137–46.
- Chong J, Soufan O, Li C, et al. MetaboAnalyst 4.0: towards more transparent and integrative metabolomics analysis. *Nucleic Acids Res.* 2018;46(W1):W486–94.
- Yu G, Wang L-G, Han Y, He Q-Y. clusterProfiler: an R package for comparing biological themes among gene clusters. *Omics J Integr Biol.* 2012;16(5):284–7.

42. Yu G, Wang LG, Yan GR, He QY. DOSE: an R/Bioconductor package for disease ontology semantic and enrichment analysis. *Bioinformatics*. 2015;31(4):608–9.
43. Chen Y, Zhang Z, Hu X, Zhang Y. Epigenetic characterization of sarcopenia-associated genes based on machine learning and network screening. *Eur J Med Res*. 2024;29(1):54.
44. Li K, Li D, Hafez B, et al. Identifying and validating MMP family members (MMP2, MMP9, MMP12, and MMP16) as therapeutic targets and biomarkers in kidney renal clear cell carcinoma (KIRC). *Oncol Res*. 2024;32(4):737–52.
45. Otasek D, Morris JH, Boucas J, Pico AR, Demchak B. Cytoscape automation: empowering workflow-based network analysis. *Genome Biol*. 2019;20(1):185.
46. Sha Z, Zhou J, Wu Y, et al. BYSL promotes glioblastoma cell migration, invasion, and mesenchymal transition through the GSK-3 β / β -catenin signaling pathway. *Front Oncol*. 2020;10:565225.
47. Jiang Y, Li S, Zhou Q, et al. PDCD4 negatively regulated osteogenic differentiation and bone defect repair of mesenchymal stem cells through GSK-3 β / β -catenin pathway. *Stem Cells Dev*. 2021;30(16):806–15.
48. Hou G, Li J, Liu W, et al. Mesenchymal stem cells in radiation-induced lung injury: from mechanisms to therapeutic potential. *Front Cell Dev Biol*. 2022;10:1100305.
49. Uccelli A, Moretta L, Pistoia V. Mesenchymal stem cells in health and disease. *Nat Rev Immunol*. 2008;8(9):726–36.
50. Azzam El, Jay-Gerin J-P, Pain D. Ionizing radiation-induced metabolic oxidative stress and prolonged cell injury. *Cancer Lett*. 2012;327(1–2):48–60.
51. Cheng L, Yu P, Li F, et al. Human umbilical cord-derived mesenchymal stem cell-exosomal miR-627-5p ameliorates non-alcoholic fatty liver disease by repressing FTO expression. *Hum Cell*. 2021;34(6):1697–708.
52. Ma Y, Wang L, Yang S, et al. The tissue origin of human mesenchymal stem cells dictates their therapeutic efficacy on glucose and lipid metabolic disorders in type II diabetic mice. *Stem Cell Res Ther*. 2021;12(1):1–15.
53. Norris GH, Blesso CN. Dietary and endogenous sphingolipid metabolism in chronic inflammation. *Nutrients*. 2017;9(11):1180.
54. El Ridi R, Duan J, Jin J. Editorial: sphingolipid metabolism dysfunction in cancer. *Front Endocrinol*. 2023;14:1208616.
55. Alaamery M, Albeshar N, Aljawini N, et al. Role of sphingolipid metabolism in neurodegeneration. *J Neurochem*. 2021;158(1):25–35.
56. Jia L, Jiang Y, Wu L, et al. *Porphyromonas gingivalis* aggravates colitis via a gut microbiota-linoleic acid metabolism-Th17/Treg cell balance axis. *Nat Commun*. 2024;15(1):1617.
57. Mercola J, D'Adamo CR. Linoleic acid: a narrative review of the effects of increased intake in the standard American diet and associations with chronic disease. *Nutrients*. 2023;15(14):3129.
58. Campos AM, Maciel E, Moreira AS, et al. Lipidomics of mesenchymal stromal cells: understanding the adaptation of phospholipid profile in response to pro-inflammatory cytokines. *J Cell Physiol*. 2016;231(5):1024–32.
59. Levental KR, Surma MA, Skinkle AD, et al. ω -3 polyunsaturated fatty acids direct differentiation of the membrane phenotype in mesenchymal stem cells to potentiate osteogenesis. *Sci Adv*. 2017;3(11):eaao1193.
60. Rampler E, Egger D, Schoeny H, et al. The power of LC-MS based multiomics: exploring adipogenic differentiation of human mesenchymal stem/stromal cells. *Molecules*. 2019;24(19):3615.
61. Gao S, Sha Z, Zhou J, et al. BYSL contributes to tumor growth by cooperating with the mTORC2 complex in gliomas. *Cancer Biol Med*. 2021;18(1):88–104.
62. Itoh H, Nishikawa S, Haraguchi T, et al. Aldehyde dehydrogenase activity helps identify a subpopulation of murine adipose-derived stem cells with enhanced adipogenic and osteogenic differentiation potential. *World J Stem Cells*. 2017;9(10):179–86.
63. Aikio E, Koivukoski S, Kallio E, et al. Complementary analysis of proteome-wide proteomics reveals changes in RNA binding protein-profiles during prostate cancer progression. *Cancer Rep*. 2023;6(10): e1886.
64. Li Y, Fu H, Wang H, et al. GLP-1 promotes osteogenic differentiation of human ADSCs via the Wnt/GSK-3 β / β -catenin pathway. *Mol Cell Endocrinol*. 2020;515:110921.

Publisher's Note

Springer Nature remains neutral with regard to jurisdictional claims in published maps and institutional affiliations.